Dual-Mode Cooperative Binding of Adenosine 5′-Triphosphate to Poly(L-lysine)†

Gerhard Schwarz* and Thomas J. Gilligan III

ABSTRACT: Equilibrium dialysis studies of adenosine triphosphate interacting with polylysine at low polymer concentration yield Scatchard plots exhibiting an apparent noncooperative binding mode superimposed on a positively cooperative one. The same behavior has been reported in the literature for various mononucleotides and basic poly(amino acids). It is pointed out here that both modes must not be considered as independent but to be mutually exclusive. Applying a pertinent theoretical approach yields higher degrees of cooperativity than obtained for mutual independence. Another necessary modification in the analysis of data takes into account that one ligand interacts with more than one equivalent binding contact (i.e., an elementary charge here). This leads to a further enhancement of the actual cooperativity. Increasing the polymer concentration in the binding experiments reveals a cooperative effect also in the first binding mode. This is physically interpreted and theoretically analyzed in terms of bound dimers stabilized by base stacking.

ATP in aqueous solution has been shown to form dimeric and even higher oligomeric aggregates due to stacking interactions between the bases. The association constant is, however, not very large so that the phenomenon only occurs at fairly high concentration (Heyn and Bretz, 1975). The nucleotide molecules can be expected to aggregate more strongly if a positively charged polymer is added in order to neutralize at least partially the unfavorable electrostatic repulsion of the negative charges on the phosphate tails.

In principle, the behavior of the system can qualitatively be deduced from that of positively charged acridine dye molecules as they interact with each other and polyanions. In aqueous solution, pronounced stacking of acridine orange is observed at comparatively low concentration (Robinson et al., 1973). Upon adding poly(L-glutamic acid), charge neutralization leads to considerably enhanced aggregation of the dye along the polymer chain. This effect can be described as cooperative binding of a small ligand to a linear lattice of binding sites (Schwarz, 1970; Schwarz and Balthasar, 1970). When the overall charge is largely neutralized on the dye–polymer complexes, these themselves combine to form larger aggregates which may even precipitate (Schwarz and Seelig-Löffler, 1975).

Analogous phenomena, to be expected with ATP (or other nucleotides) and a basic polypeptide, should not only be of significance regarding fundamental aspects of protein–nucleic acid interactions but also for an understanding of how ATP and similar molecules may be stored in biological systems (e.g., such as blood platelets or presynaptic vesicles) and how these storage functions could be manipulated.

The present article is mainly concerned with some pertinent experimental data obtained for ATP and poly(L-lysine) (mainly by equilibrium dialysis) and an approach to describe and interpret them quantitatively in terms of an appropriate theory and physical picture.

Experimental Section

The disodium salt of adenosine 5′-triphosphate has been purchased from Merck. Radioactive material ([8-^{14}C]ATP) for equilibrium dialysis obtained from NEN had a specific activity of about 50 Ci/mmol in a 1:1 ethanol–water solution. It was dried either by evaporation under vacuum or by lyophilization to remove the ethanol and could then be redissolved in the appropriate buffer.

The experimentally employed solutions were made using one of three different buffers, namely, 25 mM acetate (adjusted to pH 5.3 or 7.0), 50 mM cacodylate (pH 7.5), and 50 mM Tris[1] (pH 7.5). The nucleotide concentrations could be determined from their optical absorbance at 260 nm or in case of the labeled substances from their activities.

Two lots of poly(L-lysine) supplied by Miles-Yeda (LY 50: mol wt 26 300; LY 164: mol wt 30 000) as the bromide salt were used. The polymer was dialyzed exhaustively against the buffer to remove counterions and possible small chain impurities. Its concentration was determined by means of the ninhydrin method (Moore and Stein, 1954) using a leucine standard.

The equilibrium dialysis experiments were conducted with cells made available by K. Kirschner of this department. They have a volume of 200 μL on each side of the membrane. The membrane is a Sartorius SM 115-39 made of regenerated cellulose having a pore size of 50 Å and absolutely impermeable for the polypeptide, as demonstrated by negative ninhydrin tests of samples taken from the pure ATP side. The membranes were stored in 30% ethanol–water and then preequilibrated in the buffer (changed several times) for 30 min before use. They were blotted dry before assembly into the cell. One side was then filled with polymer (100 μL). The other side was first filled with labeled nucleotide (50 μL) and then with varying much larger concentrations of nucleotides. The cells were finally placed in a rotating temperature-controlled device and allowed to equilibrate for at least 4 h. Studies of the time dependence showed equilibrium to be attained in 2 h. Each cell contains two separate dialysis chambers. Duplicates were run in the same cell. Sampling and filling were carried out using Hamilton syringes with Chaney adaptor, and normally a 50-μL sample was taken for analysis.

The radioactive sample was then placed in 0.5 mL of ethanol in a plastic counting vial. Then, 10.0 mL of counting solution

† From the Department of Biophysical Chemistry, Biocenter of the University of Basel, Basel, Switzerland. *Received June 30, 1976.* This research was supported by Grant 3.150.73 of the Swiss National Science Foundation.

[1] Abbreviations used are: Tris, 2-amino-2-hydroxymethyl-1,3-propanediol; Me_2POPOP, 2,2′-*p*-phenylenebis(4-methyl-5-phenyloxazole); PPO, 2,5-diphenyloxazole.

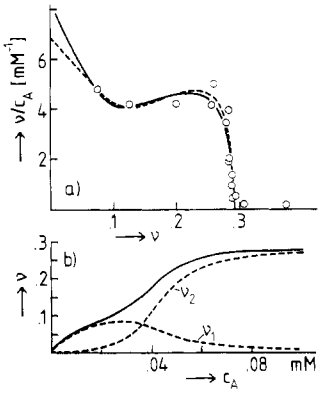

FIGURE 1: Binding of ATP to 1.72 mM polylysine at pH 7.5 (50 mM cacodylate) and 25 °C. (a) Measured Scatchard plots and theoretical curve fits according to models described in Table II and discussed in the text. (b) Individual and overall binding curves corresponding to the solid curve in the above diagram.

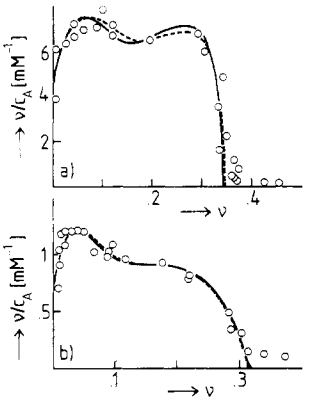

FIGURE 2: Scatchard plots of ATP binding to more concentrated polylysine. Theoretical curve fits according to models described in Table II and discussed in the text. (a) Polymer concentration 6.33 mM at pH 7.0 (25 mM acetate) and 25 °C. (b) Polymer concentration 7.12 mM at pH 5.3 (25 mM acetate) and 25 °C.

(made of 66 mL of ethanol, 5 g of PPO, 0.3 g of Me_2POPOP diluted with toluene to make 1 L) was added, and the contents were shaken and counted in the ratio mode using the external standard to correct for quenching in a Packard Counter Model 3325. Binding reversibility was checked by approaching data points at increasing as well as decreasing concentrations of the ligand.

In cases where turbidity occurred on the polymer side, only the side with no polymer was sampled and the amount bound was calculated from the amount initially present. Attempts at sampling the polymer side in such cases resulted in a lower than expected total activity and great irreproducibility.

Circular dichroism spectra were determined with a Cary 61 instrument. The nucleotide–polymer ratios have been chosen smaller than those where turbidity would occur. Fluorescence measurements were carried out using a Schoeffel RRS 100 fluorimeter.

Results

In order to avoid Donnan effects, experiments were first performed at a fairly low concentration of the polymer (i.e., at about 1–2 mM). This had only the disadvantage that the measured data became rather uncertain in the range of low ligand binding. A typical Scatchard plot (at pH 7.5) is presented in Figure 1a. The points evaluated for a ν (= bound ligand per peptide unit) below about 0.07 scatter appreciably and are therefore not inserted. There is, however, a clear upward trend toward the ordinate axis. Generally all the plots obtained at such low concentration of polylysine exhibited similar shapes, namely, a gradually decaying first part followed by a convexly curved one with a hump in it which then turns down rather abruptly. Similar behavior has been observed with mononucleotides and basic polypeptides, particularly GMP and poly(L-arginine) (Wagner, 1969).

In later experiments, the polymer concentration was increased so that the low-binding part of the Scatchard plot could be determined more accurately. A typical result (pH 7.0) is given in Figure 2a. Unexpectedly, it turned out that there is definitely a decay of the curve at very low binding. This is also the case at a lower pH of 5.3, where the ATP has only 3 negative charges instead of 4 (pertinent p$K \approx 6.5$). A corresponding plot is given in Figure 2b. At these higher polymer concentrations (of about 6–7 mM) and with an acetate buffer of 25 mM, the Donnan effect can no longer be completely neglected. It should result in somewhat larger ν/c_A (c_A = concentration of free ligand). However, this can be estimated to lead to errors of no more than 10% at low ATP concentrations, where it must be expected to have the most unfavorable influence. Since this correction is also of the order of the measuring inaccuracy, it does not essentially change the plots as they are evaluated from the dialysis data. We note that the accuracy is sufficient for the intended attempt of a general mechanistic interpretation of the observed binding phenomenon. We did not increase the buffer concentration because the addition of more electrolyte generally decreases the binding affinity.

At the concentrations used in the equilibrium dialysis measurements, turbidity occurs when the ratio of ATP to polymer approaches a value close to overall charge neutralization of the nucleotide–polylysine complex (this might even result in precipitation). The turbidity also depends on pH as well as on the concentrations of electrolyte (buffer) and polymer. The effect is apparently due to the formation of larger aggregates of the ligand–polymer complexes analogous to those observed in other systems involving stacking ligands bound by oppositely charged polyions (Schwarz and Seelig-Löffler, 1975). For the equilibrium dialysis this aggregation is not a problem because the binding is reversible and equilibrium is established. Turbidity, however, naturally interferes with optical measurements.

Some preliminary fluorescence studies with ϵ-ATP (which is a fluorescent analogue of ordinary ATP) indicate that in a concentration range below about 5 μM no turbidity problem exists. On the other hand, the fluorescence signal (after correction for light scattering) still allows evaluation of the binding data. This appears to be a convenient optical method for future binding studies.

Measurements of circular dichroism have also been attempted. Unfortunately the turbidity prevented gathering more than qualitative information. There seems to be a change in the conformation of the polymer upon the addition of nucleotide. At pH 7.5, polylysine exists in an extended random-coil form exhibiting a strong positive signal at 218 nm. With added nucleotides the CD signal changes toward that of the helical form which is strongly negative at that wavelength. The magnitude of this effect decreases in the order of going from ATP to ADP, AMP, and cAMP.

Discussion

A more detailed treatment of the theoretical approaches to

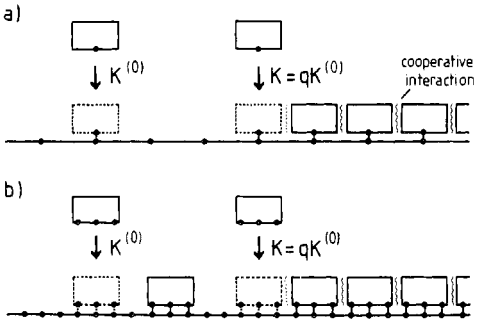

FIGURE 3: Schematic illustration of single mode binding on a linear polymer with cooperative interaction between immediate neighbors. The equilibrium constant for a nucleation step (i.e., formation of an isolated bound ligand) is K^0, for a propagation step (i.e., adjoining an already bound ligand) it is $K = qK^0$ (q being determined by the cooperative interaction). (a) Single contact binding ($n = 1$): potential binding sites do not overlap. The minimum size gap between bound ligands corresponds to one site. (b) Multiple contact binding ($n > 1$): potential binding sites overlap each other. The minimum size gap is smaller than one site ($= 1/n$).

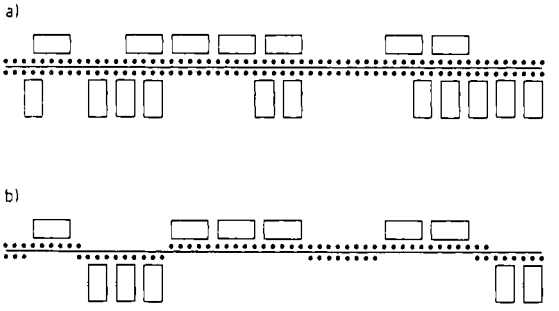

FIGURE 4: Schematic illustration of dual-mode cooperative binding models. The first mode ($n_1 = 5$) is represented above the binding lattice, the second one ($n_2 = 3$) below. (a) Independence of binding modes. (b) Mutual exclusion of binding modes. Once binding occurs (no matter which mode is effective) binding contacts for the other mode are extinguished.

linear binding and its Scatchard plots can be found elsewhere (Schwarz, 1977).

General Aspects. The binding behavior of the system under consideration will be quantitatively described in terms of a model mechanism which is as simple as possible but still physically reasonable. This may involve one or more specific binding modes. By such a mode we mean a class of ligand–polymer complexes where the binding sites are equivalent and binding parameters for any ligand are equal. However, the Scatchard plots observed in our investigation can never be explained by ordinary noncooperative binding, even if two or more different modes are superimposed. In fact, the hump which always occurs at higher ν values reflects a very pronounced degree of positive cooperativity (Schwarz, 1976).

The principal points of our analysis may be summarized as follows.

(1) The simplest cooperative binding mechanism on a linear polymer assumes one mode of binding, limits cooperative interaction to nearest neighbors, and has single contacts. The latter means that potential binding sites do not overlap. They are either completely occupied or vacant (see Figure 3a). The binding parameters are K^0, the nucleation binding constant (i.e., for binding a ligand to a site with no occupied nearest-neighbor sites), q, a cooperativity parameter, and g, the maximum number of bound ligands per polymer subunit. When dealing with larger ligands it may be more appropriate to describe binding sites as being made up by n successive equivalent binding contacts (McGhee and von Hippel, 1974) (see Figure 3b). These could correspond to individual polymer subunits where several of them are involved in the binding of one ligand. In any such binding mechanism, potential binding sites can overlap so that partial vacancy is feasible. This multiple-contact binding has essentially the same effect as negative cooperativity.

(2) The Scatchard plots resulting from our measurements cannot be understood on the basis of just one mode of binding. In principle, they may be fitted by assuming two different independent modes. However, such independence is quite unlikely because of the presumably electrostatic nature of the binding affinity. Although either potential mode of binding may occur anywhere on the completely unoccupied parts of the polymer, both will not be possible simultaneously at the same point. This is because one binding mode already neutralizes so much charge that any additional binding is virtually excluded. In other words, we have mutual exclusion of the different modes (see Figure 4).

(3) The low-concentration data as presented in Figure 1 resemble results obtained earlier with certain mononucleotides and basic polypeptides (Wagner, 1969). These can be interpreted in terms of a noncooperative mode together with a positively cooperative one. However, in contrast to the earlier assumptions of independence and single contacts we have taken into account mutual exclusion as well as multiple contact binding. With these assumptions the cooperativity is increased considerably but nucleation binding constants are decreased. The two modes are associated with binding structures, the first of them involves a most favorable interaction between ligand and polymer at the expense of base stacking, whereas the second one allows an optimum of stacking-induced cooperativity but can only result in a reduced nucleation binding constant.

(4) The positive initial slope of our Scatchard plots observed at higher concentrations (see Figure 2) is not consistent with a first mode which lacks cooperativity. From a structural point of view there is indeed reason to believe that at least every two neighboring ligands in such a binding mode can stack together and stabilize themselves by this dimerization on the polymer. Introducing such a dimeric first binding mode into the theoretical approach does in fact describe the data quite satisfactorily.

We finally conclude that the simplest but physically reasonable binding mechanism which is sufficient to explain our experimental results must involve this dual-mode cooperativity as well as mutual exclusion and multiple contacts.

The measured binding curves can be fitted with simpler models. However, this results in the evaluation of binding parameters which may appreciably deviate from the physically significant ones.

Let us now turn to a more detailed presentation of our discussion.

Single Mode Cooperative Binding on a Linear Polymer. The basic model implies a lattice of equivalent binding sites leading to one mode of ligand–polymer complexes. The nucleation binding constant, K^0, for an isolated bound ligand is determined by the interaction between the ligand and the polymer only. When one or more neighboring sites are already occupied, the cooperative interactions will contribute to the binding constant. When such cooperative interaction is confined to immediate neighbors, the same cooperative binding constant, K, applies to any binding where one neighboring site is occupied. The ratio $q = K/K^0$ then measures the degree of coop-

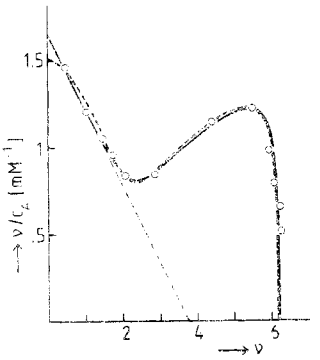

FIGURE 5: Scatchard plot of GMP binding to polylysine (about 1.5 mM) at pH 7.0 (20 mM acetate) and 0 °C after Wagner (1969). The curves have been calculated using models described in Table I and discussed in the text.

erativity ($q > 1$ or $q < 1$ characterizing positive or negative cooperativity, respectively).

Generally, the binding ratio ν can be written

$$\nu = g\theta$$

where θ stands for the fraction of occupied binding contacts and g for the number of sites per peptide unit. This degree of binding, θ, naturally equals the fraction of bound ligands (with regard to the maximum number which can be accommodated). Obviously, it may be expressed as

$$\theta = \frac{\phi}{1 + \phi}$$

if ϕ is defined as the ratio of occupied vs. unoccupied contacts. We could consider ϕ to be an apparent overall binding "constant". In general, it will be a function of the free ligand concentration and depend on the various binding parameters except g.

In the simplest case, namely, nearest-neighbor cooperativity and single-contact binding, we have

$$\phi = (\xi + \sqrt{1 + \xi^2})^2$$

with

$$\xi = \sqrt{q}(s - 1)/(2\sqrt{s})$$

where $s = Kc_A$.

If n binding contacts are assumed, the more general expression applies

$$\phi = (nq/s)(\lambda - 1)^2\lambda^{n-1}$$

where λ has to be calculated as the largest root of the algebraic equation

$$q(x - 1)(x^n - s) = s$$

A computer program for λ can be based on the apparent fact that there is always one and only one root above unity.

Using ϕ we can calculate θ and then ν for any c_A at given K^0, q, n, and g. Furthermore

$$\nu/c_A = gK(\theta/s)$$

is readily accessible so that the respective Scatchard plot can be drawn. A detailed inspection shows that these plots cannot clearly differentiate values of q and n. As a first approximation, we obtain practically the same plot for the same ratio of q/n at constant values of $K(= qK^0)$ and g. In other words, an increase in the number of contacts can be compensated for by a similar increase in cooperativity for the observed binding behavior.

It turns out that nearest-neighbor cooperativity in single mode binding never results in a distinct turning point of the Scatchard plot as found in our data. In principle, this would be possible if cooperative interaction occurs beyond nearest neighbors. However, the big hump at high ν would then imply that more distant ligands exert a much stronger (positive) cooperativity than nearer ones. Actually, this appears quite unlikely since the short-range effect of base stacking is the only apparent source of positive cooperativity, whereas the long-range electrostatic effects produce negative cooperativity. We therefore discount any single-mode binding mechanism for the present system.

A Basic Dual Mode Binding Model. Assuming two binding modes yields

$$\nu = g_1\theta_1 + g_2\theta_2; \qquad \frac{\nu}{c_A} = g_1K_1\left(\frac{\theta_1}{s_1}\right) + g_2K_2\left(\frac{\theta_2}{s_2}\right)$$

where θ_i represents the fraction of bound ligands according to mode i and $s_i = K_ic_A$ (g_i, $K_i = q_iK_i^0$ being the respective binding parameters as introduced before).

If the different modes are completely independent of each other, we evidently have

$$\theta_i = \frac{\phi_i}{1 + \phi_i}$$

with the respective ϕ function given above. However, such independence of binding modes must not be assumed in our case. As was pointed out already, we have to take into account the mutual exclusion effect. Its rigorous treatment leads to computational difficulties so that a simple approximation yielding

$$\theta_i = \frac{\phi_i}{1 + \phi_1 + \phi_2}$$

may be used (Schwarz, 1977).

We turn now to the type of Scatchard plot shown in Figure 1. Similar ones have been observed with related mononucleotides and basic polypeptides as mentioned before. An example for GMP and polylysine is given in Figure 5. In his analysis the author did not consider multiple contacts and assumed an independent superposition of a noncooperative mode (with $q_1 = 1$, $K = K_1^0$) which was responsible for the initial negative slope of the plot and a positively cooperative mode ($q_2 > 1$) reflected in the hump. This can indeed describe the data quite satisfactorily. Binding parameters evaluated on this basis are presented in Table I.

From the structural point of view a dual mode binding of this kind is readily conceivable. We propose that in the first mode optimum binding strength of an isolated nucleotide–polymer complex is achieved, implying a comparatively high value of K_1^0 at the expense of base stacking so that there is no cooperativity. On the other hand, there is a second mode of comparatively weak ligand–polymer binding (i.e., low K_2^0) which allows optimum stacking of bases so that extended aggregates of bound ligands are stabilized by cooperative interaction. These properties are indeed already consistent with the parameters evaluated by Wagner except that one finds $g_2 < g_1$. In the light of our proposed stacking, in the second mode less separation of ligands would be physically reasonable, thus $g_2 > g_1$. In fact, this turns out to be the case if mutual exclusion is taken into account as can be seen from the pertinent parameters evaluated in Table I. We also call attention to the appreciably increased q_2 and the correspondingly decreased

TABLE I: Binding Parameters of GMP/Polylysine Data (Figure 5) Measured by Wagner (1969) According to Various Dual Mode Binding Models Discussed in the Text.

Model	K_1^0 (mM^{-1})	q_1	$g_1(n_1)$	K_2^0 (K_2) (mM^{-1})	q_2	$g_2(n_2)$
Independent modes, single contacts	4.4	1	0.38	0.09 (2.9)	33	0.25
Mutual exclusion, single contacts	4.4	1	0.38	0.019 (2.8)	150	0.63
Mutual exclusion, multiple contacts (solid curve)	1.65	1	0.53 (1.9)	0.011 (2.7)	245	0.63 (1.6)
Mutual exclusion, multiple contacts (dashed curve)	1.5[a]	3[a]	0.4 (2.5)[a]	0.0115 (2.8)	245	0.63 (1.6)

[a] Dimeric mode.

TABLE II: Binding Parameters of ATP/Polylysine Data Presented in this Article (Figures 1 and 2) According to Various Dual-Mode Mutual Exclusion Models Discussed in the Text.

System Model	K_1^0 (K_1) (mM^{-1})	q_1	$g_1(n_1)$	K_2^0 (K_2) (mM^{-1})	q_2	$g_2(n_2)$
Single contacts (dashed curve)[b]	30	1	0.225	0.5 (25)	50	0.295
Multiple contacts (solid curve)[b]	8	1	0.24 (4)	0.25 (25)	100	0.294 (3.4)
Single contacts (dashed curve)[c]	15 (135)[a]	9[a]	0.26[a]	0.62 (31)	50	0.35
Multiple contacts (solid curve)[c]	3.8 (145)[a]	38[a]	0.26 (3.8)[a]	0.23 (32)	140	0.35 (2.9)
Single contacts (dashed curve)[d]	4 (50)[a]	12.5[a]	0.12[a]	0.5 (6.3)	12.6	0.37
Multiple contacts (solid curve)[d]	0.5 (44)[a]	88[a]	0.14 (7)[a]	0.175 (5.8)	33	0.33 (3.05)

[a] Dimeric modes. [b] Figure 1. [c] Figure 2a. [d] Figure 2b.

K_2^0 (K_2 remains practically unchanged). This can be interpreted as follows. At c_A below about $1/K_2$ only the first mode contributes appreciably to ν. Then the cooperative mode sets in rather abruptly so that K_2 is associated with the turning point in the Scatchard plot. In the mutual exclusion model the first mode is largely suppressed at higher ν (see Figure 1b) and the second mode almost exclusively determines the hump. An appropriate curve fit thus needs a greater q than was required under the assumption of independent modes. In the latter case also the first mode contributes to the hump so that less positive cooperativity is necessary. From the g factors we gather that 2.6 and 1.6 lysine units, respectively, are involved in a binding site (note that GMP bears two negative charges compared with a positive one on the peptide unit). Therefore, multiple contact binding appears to be quite appropriate here. We associate one peptide unit with a basic binding contact and set $g_i = 1/n_i$. Under these circumstances, we obtain again a modified set of binding parameters (with further enhanced q_2), where those for the first mode are also affected (see Table I).

Our ATP/polylysine data of Figure 1a have been treated in the same way. The respective parameters can be found in Table II.

The evaluation procedure is readily conducted using a simple programmable desk calculator, preferably equipped with a plotter. One may feel that fitting the data on the basis of our theoretical expressions would lead to a great deal of uncertainty in the five adjustable parameters. However, this is not the case if the two different phases of the Scatchard plot are distinctly recognizable and experimentally determined with some accuracy. We note that the individual parameters largely depend on rather different properties of the plot. In our present model that includes mutual exclusion and multiple contacts, the intercept on the ordinate is approximately equal to K_1^0, while extrapolating the initial slope to the abscissa (see Figure 5) yields about $1/(2n_1 - 1)$. The parameters K_2, q_2, and n_2, on the other hand, are mainly determined by the turning point of the plot (there we have $K_2c_A \approx 1$), the height of the hump, and the final intercept on the abscissa ($\nu_2 \to \approx 1/n_2$), respectively. In this way we obtain approximate values which can be refined by an appropriate curve-fitting procedure.

Dimerization in the First Binding Mode. Our measurements with higher concentrations of ATP and polylysine (see Figure 2) have clearly shown an initial steep positive slope of the Scatchard plot. This is absolutely incompatible with a noncooperative first mode as discussed above. The binding of the first ligand according to the first mode must be weaker than so far observed, but there is now a pronounced positively cooperative interaction associated with the binding to a neighboring site (Schwarz, 1976). This type of cooperative binding is, however, unlikely to result in long cooperatively bound stacks as would be the case with the second mode. Such behavior would necessarily lead to an abrupt decrease in the plot after the maximum. Although this behavior cannot be absolutely excluded when inspecting the data, the physical picture behind our binding mechanism disfavors it very much.

We may point to the fact that ATP alone can form rather stable dimers if only the electrostatic repulsion forces between monomers are sufficiently reduced (Gilligan and Schwarz, 1976). It is thus easily conceivable that a first ATP molecule bound to the oppositely charged polymer allows another one to bind much better at a neighboring site by taking advantage of the stacking of the bases. Further stacking may then be suppressed because of an unfavorable geometry of the complex. Since appreciable cooperative oligomerization has already been excluded, we shall assume for the sake of simplicity that only dimers occur.

A quantitative treatment of the dimeric binding mode may be developed using the so-called sequence generating functions method (Lifson, 1964; Schwarz, 1977). The nucleation binding constant is again denoted K^0, whereas $K = qK^0$ stands for the binding constant for the formation of a bound dimer (the binding constant for the second neighbor would then be again K^0, for the third one K, and so forth). With $s_0 = K^0c_A$, application of the pertinent mathematical procedure yields

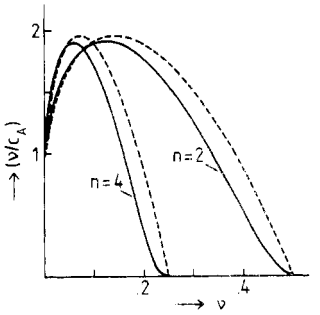

FIGURE 6: Theoretical Scatchard plots for the pure dimeric binding mode (see text). The solid curves refer to the multiple-contact concept and $K^0 = 1$. The parameters q, g are 20, 0.5 ($n = 2$), and 40, 0.25 ($n = 4$), respectively. At the same g values the one-contact approach yields the dashed curves using a K^0 and q multiplied or divided by n, respectively, namely, 2, 10, and 4, 10 (implying an apparent increase of K^0 and decrease of q).

$$\phi = \frac{\alpha - (1 + 2s_0)}{\sqrt{\alpha} + (1 + 2s_0)}$$

with $\alpha = 1 + 4s_0(1 + qs_0)$.

This, however, does not yet take into account the multiple-contact effect. Scatchard plots for a pure dimeric mode of this type are shown in Figure 6 (dashed curves). They look quite similar to the initial phases of our experimental plots in Figure 2. Indeed, a combination of this dimeric mode with a standard positively cooperative binding mode can well describe the data (dashed curves in Figure 2). The parameters are presented in Table II. Approximate values applicable to a corresponding multiple-contact binding model can be derived from these in the way mentioned above. Applying the sequence generating functions method to contacts instead of sites the appropriate ϕ function comes out as

$$\phi = ns_0 \frac{\lambda^{n-1} + 2qs_0}{\lambda^{n-1}(\lambda^n + s_0)}$$

where $\lambda(>1)$ is the largest root of

$$x^{n-1}[x^n(x - 1) - s_0] = qs_0^2$$

Again there is one and only one root above unity. Scatchard plots of such binding alone are also shown in Figure 6 (solid curves). At the present stage such a dimeric first mode together with a standard cooperative mode seems the most reasonable for analyzing the ATP/polylysine binding experiments. Solid curves fitting the data are presented in Figure 2. The individual parameters can be found in Table II.

The cooperativity of the dimeric binding step turns out to be quite pronounced (in contrast to the GMP/polylysine system where q_1 hardly exceeds a value of 3, see Figure 3 and Table I). Note that q_1 increases with decreasing pH, whereas q_2 falls. This is quite consistent with the behavior of pure ATP regarding dimerization and oligomerization, respectively (Gilligan and Schwarz, 1976).

According to our results the second mode involving longer stacks of adenine bases will be associated with about three lysine residues per nucleotide. This parallels the tendency to neutralize charges but is hard to envisage as a binding structure which retains the original stretched random-coil conformation of the polylysine chain. The polymer apparently must assume a comparatively compressed form upon binding of the ligand (at least if bound in the second mode). This is confirmed by the CD measurements mentioned before.

There are still some experimental points which obviously fall outside the theoretical analysis so far given. We refer to the scattered ones at high ligand concentration. These must be due to at least one additional but rather weak binding possibility for the ATP which may be disregarded for the present.

References

Gilligan, T. J., III, and Schwarz, G. (1976), *Biophys. Chem. 4*, 55-63.

Heyn, M. P., and Bretz, R. (1975), *Biophys. Chem. 3*, 35-45.

Lifson, S. (1964), *J. Chem. Phys. 40*, 3705-3710.

McGhee, J. D., and von Hippel, P. H. (1974), *J. Mol. Biol. 86*, 469-489.

Moore, S., and Stein, W. H. (1954), *J. Biol. Chem. 211*, 907-913.

Robinson, B. H., Löffler, A., and Schwarz, G. (1973), *J. Chem. Soc., Faraday Trans. 1 69*, 56-69.

Schwarz, G. (1970), *Eur. J. Biochem. 12*, 442-453.

Schwarz, G. (1976), *Biophys. Struct. Mech. 2*, 1-12.

Schwarz, G. (1977), *Biophys. Chem. 6*, 65-76.

Schwarz, G., and Balthasar, W. (1970), *Eur. J. Biochem. 12*, 461-467.

Schwarz, G., and Seelig-Löffler, A. (1975), *Biochim. Biophys. Acta 379*, 125-138.

Wagner, K. G. (1969), *Eur. J. Biochem. 10*, 261-267.